HETEROCYCLES, Vol. 102, No. 2, 2021, pp. 1337 - 1353. © 2021 The Japan Institute of Heterocyclic Chemistry
Received, 26th March, 2021, Accepted, 10th May, 2021, Published online, 26th May, 2021
DOI: 10.3987/COM-21-14467

BIOLOGICAL EVALUATION AND SYNTHESIS OF THIAZOLE SCHIFF BASE DERIVATIVES

Wei Zhou, Fengyan Wu, and Jinbing Liu*

School of Food and Chemical Engineering, Shaoyang University, Shao Shui Xi Road, Shaoyang 422100, PRC; syuliujb@163.com

Abstract – In this study, we report the synthesis of thiazole Schiff base derivatives (**Z1**-**Z16**) and their tyrosinase inhibitory activity, anti-oxidant activities. Mushroom tyrosinase inhibitory assay showed compound **Z8** (IC_{50} = 2.78 ± 0.08 μM) inhibited tyrosinase more than kojic acid (49.39 ± 0.17 μM), and docking study indicated compound **Z8** (-7.32 kcal/mol) had stronger binding affinities for tyrosinase than kojic acid (-5.7 kcal/mol). Phenolic hydroxyl group on 4-position (R^2) of compound **Z8** can form Metal - Acceptor with Cu401. The results of inhibition kinetics studies demonstrated that compound **Z8** was mixed type inhibitor. The anti-browning effects manifested compound **Z8** expressed satisfactory effects in anti-browning of fresh-cut apples and fresh-cut potato. All the results indicated that thiazole Schiff base derivatives might be promising leading compounds as tyrosinase inhibitors and anti-oxidant agents.

INTRODUCTION

Tyrosinase is an oxidase containing two active metal copper ions.[1,2] Tyrosinase is a key enzyme for melanin pigment biosynthesis, it can catalyze two different reactions, including the conversion of monophenols to *o*-diphenols (monophenolase) and the conversion of *o*-diphenols to *o*-quinones (diphenolase).[3,4] Tyrosinase plays an important role in the formation of melanin in bacteria, fungi, plants and animals. Normal melanin production cannot only protect human skin from ultraviolet rays, but also reduce the damage of many toxic and harmful substances.[5] However, the production of abnormal amounts of melanin may cause aesthetic problem in humans and hyperpigmentary disorders, such as postinflammatory, hyperpigmentation, maturational dyschromia, periorbital hyperpigmentation, melasma age spots, freckles and melanoma.[6,7] In addition, tyrosinase also catalyzes the neuro-melanin production by oxidation of dopamine to dopaquinones. As excessive dopaquinones formation leads to neuronal damage and cell death, it is suggested that tyrosinase is responsible for the neuro-degeneration associated

with Parkinson's and Huntington's diseases.[8,9] For food fields, enzymatic browning of fruits and vegetables brings about fast degradation during the store and handing process. The enzymatic browning not only impairs food appearance and color, but also causes change in flavor and deficiency in nutritional values.[10] Therefore, tyrosinase inhibitors have promising applications in the agricultural sector for antibrowning of vegetables and fruits, medicinal for treatment of hyper-pigmentation disorders and cosmetic for whitening agents.[11] Kojic acid (KA) is one of the most popular depigmentation agents, however, several adverse effects have been reported as genotoxic, hepatocarcinogenic and produce allergic dermatitis.[12] Meanwhile, hydroquinone can lead to erythema, stinging, colloid milium, and allergic contact dermatitis, nail discoloration, paradoxical postinflammatory hypermelanosis.[13] Furthermore, EU (European Union) cosmetic regulations ban the use of hydroquinone and corticosteroids as skin whitening agents.[14] Thus, developments of safe, effective tyrosinase inhibitors are necessary for insecticides and anti-browning of vegetables and fruits, medicinal for treatment of hyper-pigmentation disorders and cosmetic for whitening agents.

Schiff base fragments are found in various natural, natural-derived, or synthesis compounds. Schiff base derivatives have antitumor, anticonvulsant, antiviral, antibacterial, anti-tubercular, ROS scavenging activities.[15-17] Thiazoles are an important class of heterocyclic compounds bearing sulfur and nitrogen. Thiazoles possess varied biological activities, including antimicrobial, antituberculosis, antitumor, anti-oxidant, anti-HIV, anti-inflammatory, antithrombotic, enzyme inhibition activities, and anti-allergic.[18-20] Thiazole has become a constituent of many drugs such as tiazofurin, ritonavir, ravuconazole, nitazoxanide, fanetizole, and nizatidine.[21] Thiadiazole Schiff base derivatives have been reported to display potent tyrosinase inhibitory activities in our group.[22] In light of the above observations and in a continuous effort to develop effective tyrosinase inhibitors with side effect as weak as possible, in the present study, a series of thiazole derivatives were designed and synthesized. Their inhibitory activity against mushroom tyrosinase and antioxidant activities were tested. At the same time, the structure–activity relationships of these compounds and inhibition mechanism of preferred compound were also primarily discussed. The docking study was also carried out in this paper.

RESULTS AND DISCUSSION

CHEMISTRY

The synthesis route of thiazole Schiff base derivatives was shown in Scheme **1**. 2-Amino-4-phenyl-thiazoles were synthesized from appropriate substituted α-bromoacetophenone and thiourea by ultrasound-assisted method. The thiazole Schiff base derivatives can be obtained by the condensation reaction of 2-amino-4-phenylthiazole with different benzaldehyde in ethanol. In this present study, sixteen thiazole Schiff base derivatives were synthesized. The yields of the synthesis products were

moderate to good. The synthesized compounds have been characterized by ^{1}H-NMR, ^{13}C-NMR, IR, MS. IR spectra of all compounds illustrated stretching band associated with (C=N) at about 1590 cm^{-1}. In ^{1}H-NMR spectrum, =CH proton appeared as singlet at about 9.00-9.40 ppm. Signals in the range of 6.80-8.26 ppm region belong to aromatic or thiazol protons. In ^{13}C-NMR spectrum, the signal appeared at about 171 ppm was assigned to the C=N.

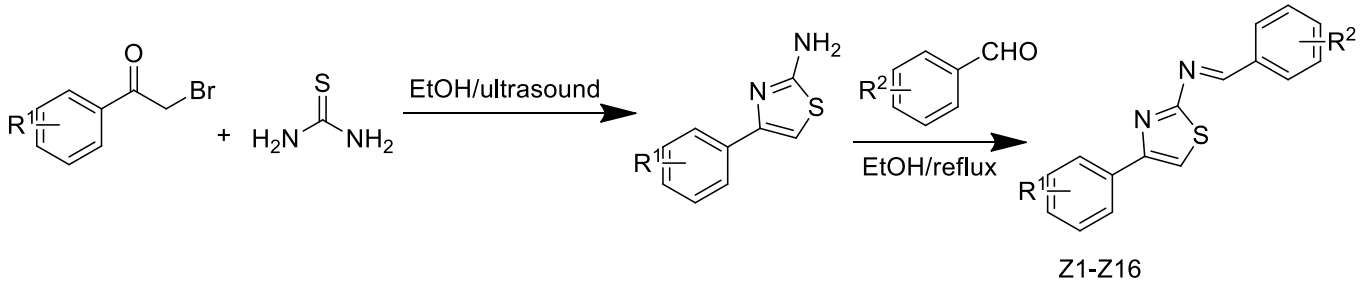

Z1 4-R^1=Cl; R^2=2-OH, 5-Cl
Z2 4-R^1=Cl; R^2=2-OH, 5-Br
Z3 4-R^1=Cl; R^2=2-OH
Z4 4-R^1=Cl; R^2=2,6 di-Br
Z5 4-R^1=Cl; R^2=2-Br
Z6 4-R^1=Cl; R^2=4-Br
Z7 4-R^1=Br; R^2=2-OH, 5-Br
Z8 4-R^1=Br; R^2=4-OH
Z9 4-R^1=Br; R^2=2-OH
Z10 4-R^1=Br; R^2=3,5 di-OMe
Z11 4-R^1=Br; R^2=4-Br
Z12 4-R^1=Br; R^2=3-Br
Z13 4-R^1=Br; R^2=3-Cl
Z14 4-R^1=OH; R$_2$=^{2}-OH, 5-Br
Z15 4-R^1=OH; R^2=2-OH, 5-Cl
Z16 4-R^1=OH; R^2=3,5 di-OMe

Scheme 1

TYROSINADE INHIBITORY ACTIVITIES

The tyrosinase inhibition measurements of compounds **Z1-Z16** were carried out using *L*-DOPA as substrate. Kojic acid was selected as a positive control compound. The inhibitory activities of the thiazol Schiff base derivatives against tyrosinase were presented in the Table **1**. Most of thiazole Schiff base derivatives showed no inhibition activity against mushroom tyrosinase at 10 mM. From the Table **1**, five compounds showed better inhibitory effects on tyrosinase than the positive control inhibitor kojic acid, and compound **Z8** was the most potent tyrosinase inhibitor with IC_{50} value of 2.78 μM ± 0.08. Compounds with the bromine atom on benzene ring (R^1) and hydroxyl on the other benzene ring (R^2) expressed more potent inhibitory activity than the other compounds and positive control inhibitor kojic acid. The results represented that the substitution type might have important influence to the inhibitory activities, and the bromine substitution might be beneficial to improve the tyrosinase inhibitory activities of the compounds. From the tyrosinase inhibitory activities of compounds **Z8, Z11**, when the hydrogen of benzene ring was replaced by the halogen atom (R^2), the inhibitory activity was disappeared. The result showed that halogen atom (R^2) may be one unfavorable factor to the increase of the inhibitory activity,

and the hydroxyl may be one favorable group. Compound **Z16** with one hydroxyl on the benzene ring (R^1) possessed better inhibitory activity than compound **Z10**. This result further illustrated the positive effect of hydroxyl group at benzene ring on the inhibitory activity.

Table 1. Tyrosinase inhibitory activity of the thiazol Schiff base derivatives

Compound	Inhibition at 10 mM (%)	IC_{50} (μM)[b]
Z1	NA[a]	---
Z2	NA	---
Z3	NA	---
Z4	15.4	>100
Z5	NA	---
Z6	NA	---
Z7	52.6	>100
Z8	98.5	2.78 ± 0.08
Z9	95.4	10.18 ± 0.11
Z10	NA	---
Z11	NA	---
Z12	NA	---
Z13	NA	---
Z14	92.5	28.17 ± 0.24
Z15	50.5	>100
Z16	93.2	37.22 ± 0.21
Kojic acid	---	43.39 ± 0.17

[a] NA = not active.

[b] Inhibitor concentration (mean of three independent experiments) required for 50% inactivation of tyrosinase.

INHIBITORY MECHANISM

Among the assessed thiazole Schiff base compounds, compound **Z8** expressed better tyrosinase inhibitory activity than the other compounds, in order to further explore the inhibition mechanism, the inhibitory type of the compound **Z8** on mushroom tyrosinase was decided by the Lineweaver–Burk double reciprocal plots. The Lineweaver–Burk plots were obtained by different concentrations of the compound **Z8** and the substrate (Figure **1A**). The inhibition type of the compound **Z8** was studied as shown in Figure **1A**. The plots of *1/V* versus *1/[S]* gave a family of straight lines with different slopes. The slope of

the curve showed downtrend with the decrease of the inhibitor concentration. All of the straight lines intersected at a point in the second quadrant. The results indicated that compound **Z8** was mixed type inhibitor. The inhibition constant (*Ki*) of the compound was obtained by a plot of the slope versus the concentrations of the compound **Z8**, *Kis* of the compound was obtained by a plot of vertical intercept ($1/V_m$) versus the concentrations of the compound **Z8**, the results were shown in the Figure **1B** and Figure **1C**. The *Ki* value and the *Kis* value of the compound were 5.02 μM and 7.81 μM, respectively. The values further demonstrated compound **Z8** could well inhibit tyrosinase activity.

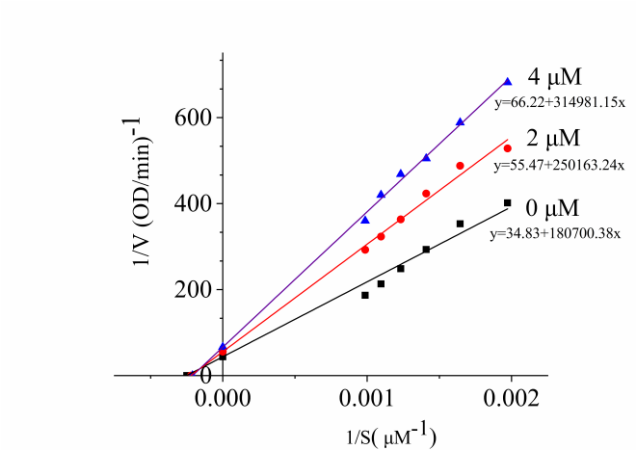

A

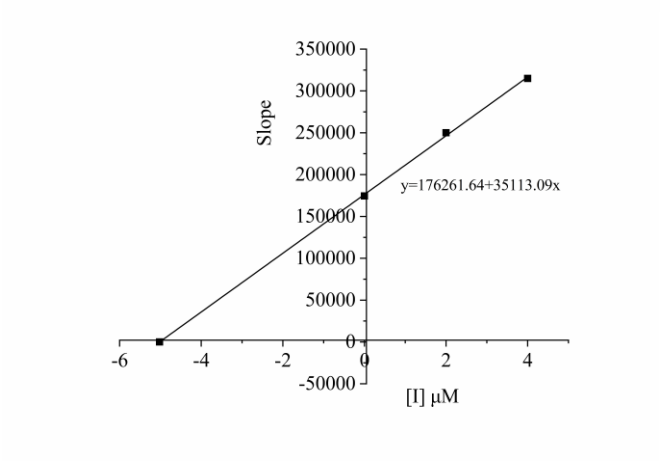

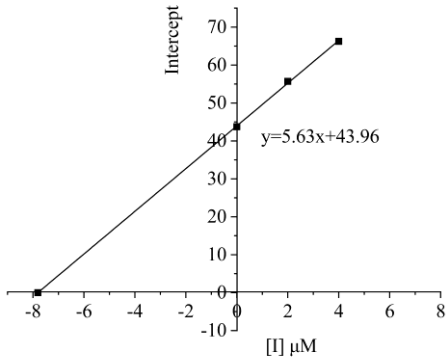

B C

Figure 1. Kinetic inhibition measurement of compound **Z8**. The type of inhibition was exhibited by Lineweavere-Burk plot. (A) The concentrations of compound **Z8** in the figure were 0, 2 μM and 4 μM, respectively. (B) The secondary replot indicates the slope versus the concentrations of compound **Z8** to define the inhibition constant Ki. (C) The secondary replot indicates the intercept versus the concentrations of compound **Z8** to define the inhibition constant Kis.

DOCKING STUDIES

The binding affinities of the compound **Z8** to the receptor tyrosinase were evaluated with computational docking study. The lower value of binding energy indicated the more stable complex was formed between the ligand and tyrosinase. The binding energy of the most active thiazole Schiff base derivative **Z8** was -7.32 kcal/mol. This compound showed higher binding affinities than kojic acid (-5.7 kcal/mol), which was used as a reference control. As shown in Figure **2**, π-π stacking interaction presented between benzene ring and His263. The same benzene ring also interacted with Ala286 and Val283 by Pi – Alkyl and Pi – Sigma, respectively. Leu275 and Pro277 can interact with bromine atom. The phenolic hydroxyl present at position 4 (R^2) in compound **Z8** can form Metal - Acceptor with Cu401. The interaction also involved in the compound **Z8** between thiazole ring and Arg268, Phe264. The nitrogen atom of Schiff base can form conventional hydrogen bond with Gly281.

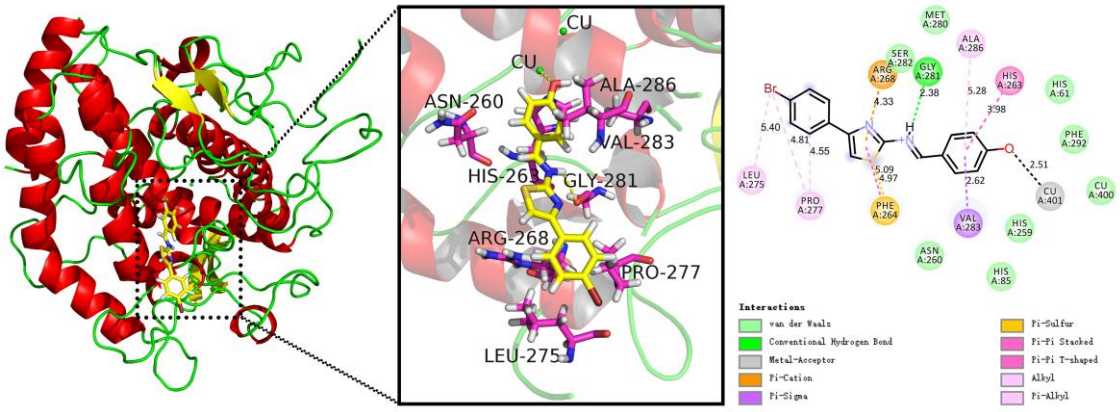

Figure 2. Ligand-protein interactions of active compound **Z8** with the active site of tyrosinase (PDB code: 2Y9X) accomplished using AutoDock4.2. The left side picture show the 3D docking of ligand in the active binding pocket with the hydrophobic effect area displayed. The medium picture shows the important interactions of atoms in the ligand with the amino acid residues of the tyrosinase. The right side figure represents the 2D interaction pattern between the ligand and protein.

FLUORESCENCE QUENCHING

Fluorescence quenching means that some small molecule compounds bind to protein that can affect the fluorescence intensity of the fluorophore. Therefore, in order to obtain information about conformational changes of enzymes, fluorescence spectroscopy has become a very important research tool. Fluorescence spectra of tyrosinase with different concentrations of compound **Z8** were investigated, as shown in Figure **3**. With increasing concentrations of compound **Z8**, the dramatically decreasing fluorescence intensity of tyrosinase could be found. This suggested the inhibitor had potent quenching effect on the fluorescence of tyrosinase. At the same time, there was no significant red shift or blue shift in the fluorescence emission

peak of tyrosinase after the addition of compound **Z8**. This result showed that the interaction between the sample and tyrosinase did not change the hydrophobic environment in the vicinity of the chromophore tryptophan residues.[23] The Stern-Volmer figure of compound **Z8** with tyrosinase at 289.15 and 304.15 K were shown in Figure **3D**. Stern-Volmer plots showed a good linear relationship, it suggested that the quenching type for compound **Z8** was single. Quenching constant decreased with increasing temperature, suggesting that the dominant quenching mechanism of compound **Z8** was a static quenching.

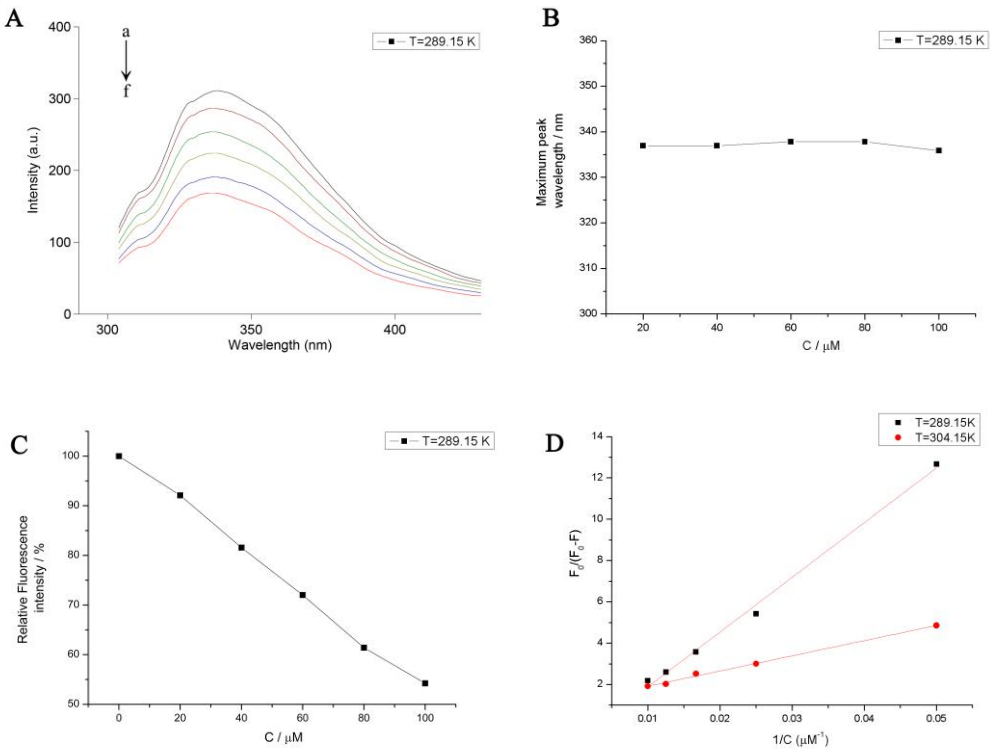

Figure 3. (A) Changes in the tyrosinase fluorescence at different concentrations of compound **Z8** (λex= 280 nm, T = 289.15 K). The final enzyme concentration was 0.1 mg/mL, and c (compound **Z8**) = 0 μM, 20 μM, 40 μM, 60 μM, 80 μM, 100 μM for the curves from top to bottom, respectively. (B) Changes in maximum peak at different concentrations of compound **Z8**. (C) Changes in fluorescence intensity at different concentrations of compound **Z8**. (D) Stern-Volmer figure of compound **Z8** and tyrosinase at 289.15 and 304.15 K.

ANTI-BROWNING STUDIES

Among the synthesized compounds, compound **Z8** showed better tyrosinase inhibitory activity. We carried out anti-browning analysis of compound **Z8** using apples and potato. In this study, kojic acid and Vc (Vitamin C) were used as positive control because they are widely applied as an anti-browning agents in the food industry. The color value change of post-cut apple treated with compound **Z8** (20 μM), blank

control group, kojic acid (40 μM) and Vc (20 μM) during storage at 5 °C was shown in Figure **4A**. The L^* values of the blank group, compound **Z8** group, kojic acid group and Vc group were 48.43, 55.26, 48.92 and 48.76, respectively, after 24 h of slicing. There were significant differences between the compound **Z8** group and blank control group, The L^* value of the compound **Z8** group was larger than positive group. During the measurement (0-24 h), the browning extent of the apple slices in the treatment group was obviously lower than the browning extent of the apple slices in the blank control group, kojic acid group and Vc group. Furthermore, in Figure **4A**, the color of the apple slices in the compound **Z8** group is lighter than the color of the positive group after 120 h of slicing. These results suggested that compound **Z8** treatment could inhibit the browning of apple slices. The changes in color values of post-cut potato treated with compound **Z8** (20 μM), blank control group, kojic acid (40 μM) and Vc (20 μM) during storage at 5 °C are presented in Figure **4B**. The L^* values of the blank group, compound **Z8** group, kojic acid group and Vc group were 53.29, 55.26, 56.86 and 56.76, respectively, after 24 h of slicing. The L^* values of the compound **Z8** group were higher than blank group. However, The L^* value of the compound **Z8** group was slightly lower than kojic acid group and Vc group. From the Figure **4B**, the L^* values of the positive control and the sample group were larger than the blank group after 120 h. In addition, L^* value of compound **Z8** was higher than positive control. The results further showed that compound **Z8** might be used as anti-browning agent.

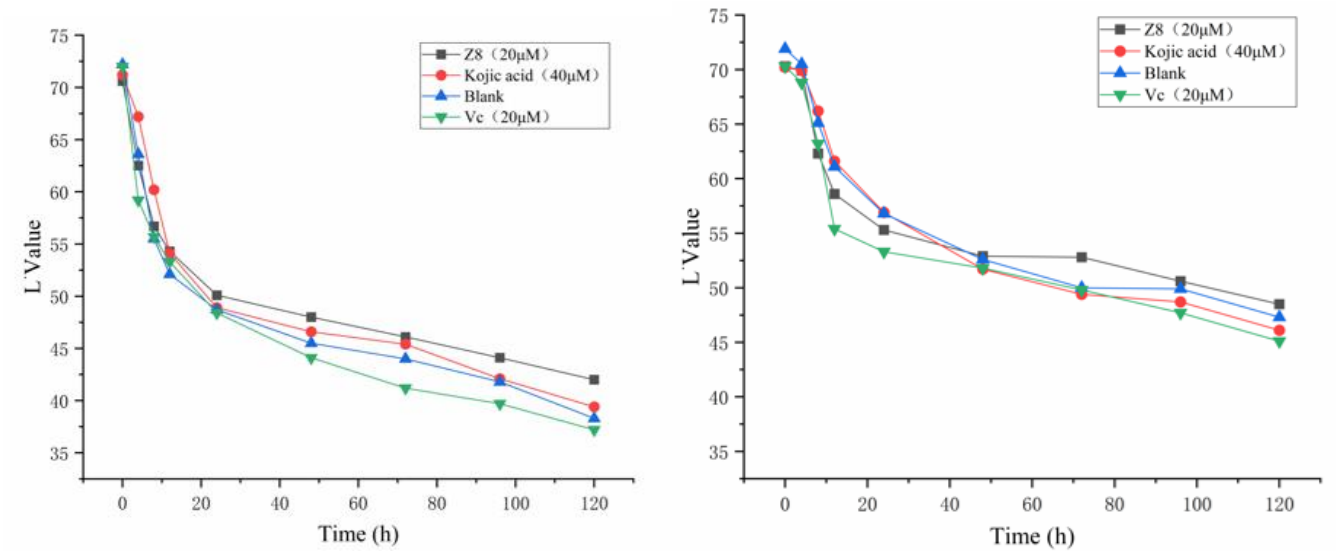

Figure 4. Effects of compound **Z8** in controlling the browning of fresh-cut apple (A) and potato slices (B) during the 120 h-storage at 5 °C.

CONCLUSIONS

In conclusion, a series of thiazole Schiff base derivatives (**Z1**-**Z16**) have been designed and synthesized as novel tyrosinase inhibitory agents, antioxidants. The most promising compound **Z8** was proved to be

potential tyrosinase inhibitor in the synthesized derivatives with the IC_{50} value of 2.78 ± 0.08 μM. It exhibited better inhibition activity than kojic acid. The inhibition kinetic study proved that compound **Z8** was mixed type inhibitor. The *Ki* value of the compound was 5.02 μM, and the *Kis* value was 7.81 μM. Molecular docking analysis exhibited that compound **Z8** (-7.32 kcal/mol) has greater binding affinities with the active site of tyrosinase than kojic acid (-5.7 kcal/mol), phenolic hydroxyl (R^2) of compound **Z8** can form Metal - Acceptor with Cu401. Phenolic hydroxyl is an essential group for activity. Fluorescence studies showed the interaction between compound **Z8** and tyrosinase did not change the hydrophobic environment in the vicinity of the chromophore tryptophan residues. The anti-browning effects manifested compound **Z8** expressed satisfactory effects in anti-browning of fresh-cut apples and fresh-cut potato. From the above results, it could be deduced that this kind of compounds can use as structural template in designing of tyrosinase inhibitors.

EXPERIMENTAL

All the reactions described below were monitored by TLC (thin layer chromatography), which was carried out with 60F254 silica gel plates. Melting points were determined using uncorrected SGW-X4 melting point apparatus. ^{1}H-NMR and ^{13}C-NMR spectra were obtained on a Bruker 400 MHz at 25 ^{o}C in DMSO-d_6 using tetramethylsilane (TMS) as an internal standard. The values of coupling constant (*J*) and chemical shift were measured in hertz (Hz) and parts per million (ppm), respectively. The abbreviations using in ^{1}H-NMR as follow: s (singlet), d (doublet), t (triplet), and m (multiplet). FT-IR spectra were recorded on a Nicolet-iS5 spectrophotometer (KBr disks). Mass-spectrometric (MS) data are reported in m/z with the LCMS-2010A. Elemental analyses were carried out using Euro EA instrument and did not exceed ± 0.04% of the theoretical values. UV-2600 spectrophotometer (Shimadzu Corporation, Tokyo, Japan) was used to record UV spectra. The fluorescence spectra of the selected compound were inspected on Cary Eclipse G9800A fluorescence spectrophotometer (Agilent Technologies Co). The colorimeter is CR-400 Minolta chronometer instrument (Konica Minolta, Osaka, Japan). Ultrasound synthesis was carried out by SB-5200DT ultrasonic cleaning machine (Ningbo Xinzhi Biotechnology Co., Ltd.) Tyrosinase, *L*-3,4-dhydroxyphenylalanine (*L*-DOPA), dimethyl sulfoxide (DMSO), dimethyl sulfoxide-d_6 (DMSO-d_6), and kojic acid were obtained from Sigma–Aldrich Chemical Co (Shanghai, China). Other chemicals were purchased from commercial suppliers.

General procedure for the synthesis of aminothiazole Schiff base (Z1-Z16)

Appropriate substituted α-bromoacetophenone (10 mmol) was dissolved in anhydrous EtOH (30 mL), and the solution was added to a single neck flask and stirred at room temperature. Then thiourea (10 mmol) was added to the above mixture. The flask was placed in ultrasonic instrument. The reaction was performed by ultrasonic method for 10-15 min at 25 ^{o}C. Frequency and intensity were 40 Hz and 300 W

respectively. The progress of reaction was tracked by thin layer chromatography (TLC). After the reaction was finished, the reaction solution was adjusted pH = 7 with ammonia water to afford precipitates. The precipitates were filtered, and then washed with 70% EtOH. The precipitates were recrystallized from EtOH.

To a mixture of aminothiazole (1 mmol) and substituted benzaldehyde (1 mmol) in EtOH (15 mL), piperidine (0.2 mL) was added. The reaction mixture was refluxed for 1-12 h. The progress of reaction was tracked by TLC. When the reaction was finished, the reaction solution was cooled to room temperature. The precipitates were filtered and washed with EtOH to afford the corresponding aminothiazole Schiff base derivatives. Some compounds were further purified by column chromatography, and the petroleum ether/EtOAc (4:1–2:1) was used as eluent.

4-Chloro-2-({[4-(4-chlorophenyl)thiazol-2-yl]imino}methyl)phenol (Z1)

Yellow solid; yield 66.4%; mp 191.4-194.3 ºC. IR (KBr), (*v* max, cm^{-1}): 3129, 1597, 1558, 1474, 1354, 1278, 1158, 1092, 1071, 1014, 933. ^{1}H-NMR (400 MHz, DMSO-*d*$_6$): 11.51 (s, 1H, -OH), 9.37 (s, 1H, =CH), 8.16 (s, 1H, Thiazol-H), 8.03 (d, *J* = 8.8 Hz, 2H, Ph-H), 7.95 (s, 1H, Ph-H), 7.55 -7.50 (m, 3H, Ph-H), 7.07 (d, *J* = 8.8 Hz, 1H, Ph-H). ^{13}C-NMR (100 MHz, DMSO-*d*$_6$): 171.2 (Thiazol C=N), 161.6 (C=N), 159.3 (Ar-OH), 151.8 (Thiazol), 134.8 (Ar-Cl), 133.3 (Ar), 133.2 (Ar), 129.3 (Ar), 128.2 (Ar), 123.9 (Ar-Cl), 121.7 (Ar), 119.4 (Ar), 115.3 (Thiazol). MS (*m/z*, I%): 348 (M^-, 100%). Anal. Calcd for $C_{16}H_{10}Cl_2N_2OS$ (349.23): C, 55.03%; H, 2.89%; N, 8.02%. Found: C, 55.06%; H, 2.93%; N, 8.04%.

4-Bromo-2-({[4-(4-chlorophenyl)thiazol-2-yl]imino}methyl)phenol (Z2)

Yellow solid; yield 62.8%; mp 206.3-208.1 ºC; IR (KBr), (*v* max, cm^{-1}): 3130, 1595, 1554, 1473, 1351, 1279, 1158, 1092, 1071, 1014, 929. ^{1}H-NMR (400 MHz, DMSO-*d*$_6$): 11.53 (s, 1H, -OH), 9.35 (s, 1H, =CH), 8.16 (s, 1H, Thiazol-H), 8.07 (d, *J* = 2.4 Hz, 1H, Ph-H), 8.03 (d, *J* = 8.8 Hz, 2H, Ph-H), 7.64 (dd, *J* = 8.8 Hz, 2.8 Hz, 1H, Ph-H), 7.55 (d, *J* = 8.8 Hz, 2H, Ph-H), 7.01 (d, *J* = 8.8 Hz, 1H, Ph-H). ^{13}C-NMR (100 MHz, DMSO-*d*$_6$): 171.3 (Thiazol C=N), 161.4 (C=N), 159.8 (Ar-OH), 151.8 (Thiazol), 137.5 (Ar-Cl), 133.2 (Ar), 132.2 (Ar), 129.4 (Ar), 129.2 (Ar), 122.3 (Ar-Br), 119.8 (Ar), 115.3 (Ar), 111.3 (Thiazol). MS (*m/z*, I%): 392 (M^-, 100%). Anal. Calcd for $C_{16}H_{10}BrClN_2OS$ (393.69): C, 48.81%; H, 2.56%; N, 7.12%. Found: C, 48.85%; H, 2.54%; N, 7.16%.

2-({[4-(4-Chlorophenyl)thiazol-2-yl]imino}methyl)phenol (Z3)

Yellow solid; yield 54.7%; mp 157.3-159.5 ºC. IR (KBr), (*v* max, cm^{-1}): 1619, 1596, 1560, 1468, 1367, 1279, 1231, 1163, 1148, 1090, 1062, 1013, 929. ^{1}H-NMR (400 MHz, DMSO-*d*$_6$): 11.57 (s, 1H, -OH), 9.40 (s, 1H, =CH), 8.14 (s, 1H, Thiazol-H), 8.03 (d, *J* = 8.8 Hz, 2H, Ph-H), 7.92 (dd, *J* = 9.2 Hz, 1.6 Hz, 1H, Ph-H), 7.55 (d, *J* = 8.8 Hz, 2H, Ph-H), 7.50 (dd, *J* = 8.8 Hz, 1.6 Hz, 1H, Ph-H), 7.04-6.99 (m, 2H, Ph-H). ^{13}C-NMR (100 MHz, DMSO-*d*$_6$): 171.3 (Thiazol C=N), 164.0 (C=N), 160.8 (Ar-OH), 151.7 (Thiazol), 135.6 (Ar-Cl), 133.3 (Ar), 131.7 (Ar), 129.4 (Ar), 128.2 (Ar), 120.3 (Ar), 120.1 (Ar), 117.4

(Ar), 114.8 (Thiazol). MS (*m/z*, I%): 314 (M^-, 100%). Anal. Calcd for $C_{16}H_{11}ClN_2OS$ (314.79): C, 61.05%; H, 3.52%; N, 8.90%. Found: C, 61.01%; H, 3.54%; N, 8.86%.

***N*-(2,6-Dibromobenzylidene)-4-(4-chlorophenyl)thiazol-2-amine (Z4)**

Yellow solid; yield 32.4%; mp 139.2-141.4 °C. IR (KBr), (*v* max, cm^{-1}): 1601, 1571, 1546, 1450, 1425, 1369, 1207, 1161, 1141, 1092, 1063, 1013, 731. ^{1}H-NMR (400 MHz, DMSO-*d*$_6$): 9.23 (s, 1H, =CH), 8.25 (s, 1H, Thiazol-H), 8.04 (d, *J* = 8.4 Hz, 2H, Ph-H), 7.86 (d, *J* = 8.4 Hz, 2H, Ph-H), 7.56 (d, *J* = 8.8 Hz, 2H, Ph-H), 7.42 (t, *J* = 8.4 Hz, 1H, Ph-H). ^{13}C-NMR (100 MHz, DMSO-*d*$_6$): 171.3 (Thiazol C=N), 162.3 (C=N), 154.7 (Ar), 152.0 (Thiazol), 138.8 (Ar), 137.6 (Ar), 133.8 (Ar-Cl), 132.3 (Ar), 131.6 (Ar), 128.5 (Ar-Br), 123.7 (Ar-Br), 122.0 (Ar), 118.1 (Thiazol). MS (*m/z*, I%): 457 (M^+, 100%). Anal. Calcd for $C_{16}H_9Br_2ClN_2S$ (314.79): C, 42.09%; H, 1.99%; N, 6.14%. Found: C, 42.12%; H, 2.03%; N, 6.13%.

***N*-(2-Bromobenzylidene)-4-(4-chlorophenyl)thiazol-2-amine (Z5)**

Yellow solid; yield 33.6% mp 105.3-107.4 °C. IR (KBr), (*v* max, cm^{-1}): 1580, 1472, 1359, 1275, 1159, 1106, 1088, 1064, 1028, 1011. ^{1}H-NMR (400 MHz, DMSO-*d*$_6$): 9.41 (s, 1H, =CH), 8.25-8.23 (m, 1H, Ph-H), 8.22 (s, 1H, Thiazol-H), 8.03 (d, *J* = 8.8 Hz, 2H, Ph-H), 7.85 (dd, *J* = 9.2 Hz, 2.8 Hz, 1H, Ph-H), 7.59-7.54 (m, 4H, Ph-H). ^{13}C-NMR (100 MHz, DMSO-*d*$_6$): 171.8 (Thiazol C=N), 162.3 (C=N), 152.0 (Ar), 135.1 (Thiazol), 134.1 (Ar), 133.3 (Ar), 133.2 (Ar-Cl), 129.7 (Ar), 129.3 (Ar), 128.9 (Ar), 128.2 (Ar), 127.2 (Ar-Br), 116.0 (Thiazol). MS (*m/z*, I%): 378 (M^+, 100%). Anal. Calcd for $C_{16}H_{10}BrClN_2S$ (377.69): C, 50.88%; H, 2.67%; N, 7.42%. Found: C, 50.86%; H, 2.65%; N, 7.42%.

***N*-(4-Bromobenzylidene)-4-(4-chlorophenyl)thiazol-2-amine (Z6)**

Yellow solid; yield 37.1%; mp 146.6-149.2 °C. IR (KBr), (*v* max, cm^{-1}): 1593, 1556, 1471, 1363, 1285, 1230, 1158, 1089, 1061, 1012, 985. ^{1}H-NMR (400 MHz, DMSO-*d*$_6$): 9.18 (s, 1H, =CH), 8.18 (s, 1H, Thiazol-H), 8.08 (d, *J* = 8.0 Hz, 2H, Ph-H), 8.03 (d, *J* = 8.0 Hz, 2H, Ph-H), 7.67 (d, *J* = 7.6 Hz, 2H, Ph-H), 7.55 (d, *J* = 7.6 Hz, 2H, Ph-H). ^{13}C-NMR (100 MHz, DMSO-*d*$_6$): 172.1 (Thiazol C=N), 163.9 (C=N), 151.9 (Thiazol), 138.2 (Ar), 134.1 (Ar-Cl), 133.9 (Ar), 132.3 (Ar), 131.9 (Ar), 129.8 (Ar), 128.5(Ar), 121.9 (Ar-Br), 115.3 (Thiazol). MS (*m/z*, I%): 378 (M^+, 100%). Anal. Calcd for $C_{16}H_{10}BrClN_2S$ (377.69): C, 50.88%; H, 2.67%; N, 7.42%. Found: C, 50.89%; H, 2.68%; N, 7.45%.

4-Bromo-2-({[4-(4-bromophenyl)thiazol-2-yl]imino}methyl)phenol (Z7)

Yellow solid; yield 58.8%; mp 208.2-210.4 °C. IR (KBr), (*v* max, cm^{-1}): 3128, 1592, 1552, 1471, 1350, 1278, 1159, 1073, 1010, 929. ^{1}H-NMR (400 MHz, DMSO-*d*$_6$): 11.53 (s, 1H, -OH), 9.35 (s, 1H, =CH), 8.17-7.67 (m, 7H, Thiazol-H, Ph-H), 7.00 (s, 1H, Ph-H). ^{13}C-NMR (100 MHz, DMSO-*d*$_6$): 171.3 (Thiazol C=N), 161.5 (C=N), 159.7 (Ar), 151.9 (Thiazol), 137.6 (Ar), 133.8 (Ar), 132.3 (Ar), 128.5 (Ar), 122.4 (Ar), 122.0 (Ar), 119.8 (Ar), 115.4 (Thiazol), 111.4 (Ar), 108.1 (Ar). MS (*m/z*, I%): 437 (M^-, 100%). Anal. Calcd for $C_{16}H_{10}Br_2N_2OS$ (438.14): C, 43.86%; H, 2.30%; N, 6.39%. Found: C, 43.84%; H, 2.32%; N, 6.41%.

4-({[4-(4-Bromophenyl)thiazol-2-yl]imino}methyl)phenol (Z8)

Yellow solid; yield 40.8%; mp 136.2-138.6 °C. IR (KBr), (*v* max, cm^{-1}): 3128, 1593, 1517, 1481, 1441, 1305, 1280, 1234, 1157, 1072, 1008, 973, 737. ^{1}H-NMR (400 MHz, DMSO-*d*$_6$): 10.51 (s, 1H, -OH), 9.00 (s, 1H, =CH), 8.04 (s, 1H, Thiazol-H), 7.95-7.91 (m, 4H, Ph-H), 7.66 (d, *J* = 8.4 Hz, 2H, Ph-H), 6.95 (d, *J* = 8.4 Hz, 2H, Ph-H). ^{13}C-NMR (100 MHz, DMSO-*d*$_6$): 173.2 (Thiazol C=N), 164.4 (C=N), 162.8 (Ar-OH), 151.5 (Thiazol), 133.9 (Ar), 132.7 (Ar), 132.2 (Ar), 128.4 (Ar), 126.5 (Ar), 121.7 (Ar-Br), 116.6 (Ar), 113.8 (Thiazol). MS (*m/z*, I%): 358 (M^-, 100%). Anal. Calcd for $C_{16}H_{11}BrN_2OS$ (359.24): C, 53.49%; H, 3.09%; N, 7.80%. Found: C, 53.52%; H, 3.11%; N, 7.81%.

2-({[4-(4-Bromophenyl)thiazol-2-yl]imino}methyl)phenol (Z9)

Yellow solid; yield 44.6%; mp 175.6-178.2 °C. IR (KBr), (*v* max, cm^{-1}): 3128, 1604, 1568, 1500, 1471, 1397, 1366, 1278, 1171, 1150, 1071, 1050, 735. ^{1}H-NMR (400 MHz, DMSO-*d*$_6$): 9.89 (s, 1H, -OH), 9.08 (s, 1H, =CH), 8.12 (s, 1H, Thiazol-H), 7.97 (d, *J* = 8.4 Hz, 2H, Ph-H), 7.67 (d, *J* = 8.4 Hz, 2H, Ph-H), 7.50-7.48 (m, 2H, Ph-H), 7.41 (t, *J* = 8.0 Hz, 1H, Ph-H), 7.07 (d, *J* = 8.8 Hz, 1H, Ph-H). ^{13}C-NMR (100 MHz, DMSO-*d*$_6$): 172.4 (Thiazol C=N), 166.2 (C=N), 158.3 (Ar-OH), 151.7 (Thiazol), 136.5 (Ar), 133.7 (Ar), 132.2 (Ar), 130.7 (Ar), 128.4 (Ar), 122.1 (Ar-Br), 121.8 (Ar), 121.0 (Ar), 115.4 (Ar), 114.8 (Thiazol). MS (*m/z*, I%): 358 (M^-, 100%). Anal. Calcd for $C_{16}H_{11}BrN_2OS$ (359.24): C, 53.49%; H, 3.09%; N, 7.80%. Found: C, 53.48%; H, 3.12%; N, 7.78%.

4-(4-Bromophenyl)-N-(3,5-dimethoxybenzylidene)thiazol-2-amine (Z10)

Yellow solid; yield 31.3%; mp 146.2-149.4 °C. IR (KBr), (*v* max, cm^{-1}): 1614, 1584, 1505, 1467, 1397, 1356, 1292, 1209, 1157, 1108, 1042, 741. ^{1}H-NMR (400 MHz, DMSO-*d*$_6$): 9.28 (s, 1H, =CH), 8.04 (s, 1H, Thiazol-H), 7.98 (d, *J* = 8.4 Hz, 2H, Ph-H), 7.85 (s, 1H, Ph-H), 7.65 (d, *J* = 8.4 Hz, 2H, Ph-H), 6.71 (d, *J* = 8.4 Hz, 2H, Ph-H), 3.95 (s, 3H, -OCH_3), 3.89 (s, 3H, -OCH_3). ^{13}C-NMR (100 MHz, DMSO-*d*$_6$): 173.6 (Thiazol C=N), 165.9 (C=N), 162.6 (Ar-O-), 158.7 (Ar-O-), 151.6 (Thiazol), 133.7 (Ar), 132.2 (Ar), 129.6 (Ar), 128.4 (Ar), 121.7 (Ar-Br), 116.1 (Ar), 113.9 (Thiazol), 107.8 (Ar), 98.6 (Ar), 56.6 (CH_3), 56.3 (CH_3). MS (*m/z*, I%): 404 (M^+, 100%). Anal. Calcd for $C_{18}H_{15}BrN_2O_2S$ (403.29): C, 53.61%; H, 3.75%; N, 6.95%. Found: C, 53.64%; H, 3.71%; N, 6.98%.

***N*-(4-Bromobenzylidene)-4-(4-bromophenyl)thiazol-2-amine (Z11)**

Yellow solid; yield 38.7%; mp 149.2-152.9 °C. IR (KBr), (*v* max, cm^{-1}): 1602, 1582, 1558, 1485, 1474, 1399, 1295, 1203, 1162, 1100, 1065, 1009, 738. ^{1}H-NMR (400 MHz, DMSO-*d*$_6$): 9.16 (s, 1H, =CH), 8.16 (s, 1H, Thiazol-H), 8.01 (d, *J* = 8.8 Hz, 2H, Ph-H), 7.96 (d, *J* = 8.4 Hz, 2H, Ph-H), 7.80 (d, *J* = 8.8 Hz, 2H, Ph-H), 7.68 (d, *J* = 8.8 Hz, 2H, Ph-H). ^{13}C-NMR (100 MHz, DMSO-*d*$_6$): 172.1 (Thiazol C=N), 164.0 (C=N), 151.8 (Thiazol), 134.3 (Ar), 133.6 (Ar), 132.7 (Ar), 132.2 (Ar), 131.9 (Ar), 128.4 (Ar), 127.3 (Ar-Br), 121.9 (Ar-Br), 115.3 (Thiazol). MS (*m/z*, I%): 423 (M^+, 100%). Anal. Calcd for $C_{16}H_{10}Br_2N_2S$ (422.14): C, 45.52%; H, 2.39%; N, 6.64%. Found: C, 45.53%; H, 2.36%; N, 6.67%.

***N*-(3-Bromobenzylidene)-4-(4-bromophenyl)thiazol-2-amine (Z12)**

Yellow solid; yield 45.0%; mp 143.3-145.6 ºC. IR (KBr), (*v* max, cm^{-1}): 1593, 1558, 1468, 1398, 1363, 1285, 1231, 1159, 1074, 1062, 1010, 743. ^{1}H-NMR (400 MHz, DMSO-d_6): 9.16 (s, 1H, =CH), 8.24 (s, 1H, Ph-H), 8.18 (s, 1H, Thiazol-H), 8.08 (d, *J* = 8.0 Hz, 1H, Ph-H), 7.97 (d, *J* = 8.8 Hz, 2H, Ph-H), 7.84 (d, *J* = 8.8 Hz, 1H, Ph-H), 7.68 (d, *J* = 8.8 Hz, 2H, Ph-H), 7.56 (t, *J* = 8.0 Hz, 1H, Ph-H). ^{13}C-NMR (100 MHz, DMSO-d_6): 171.8 (Thiazol C=N), 163.6 (C=N), 151.9 (Thiazol), 137.4 (Ar), 135.9 (Ar), 133.6 (Ar), 132.4 (Ar), 132.2 (Ar), 131.7 (Ar), 129.1 (Ar), 128.4 (Ar-Br), 122.8 (Ar-Br), 121.9 (Ar), 115.5 (Thiazol). MS (*m/z*, I%): 423 (M^+, 100%). Anal. Calcd for $C_{16}H_{10}Br_2N_2S$ (422.14): C, 45.52%; H, 2.39%; N, 6.64%. Found: C, 45.55%; H, 2.37%; N, 6.61%.

4-(4-Bromophenyl)-*N*-(3-chlorobenzylidene)thiazol-2-amine (Z13)

Yellow solid; yield 32.0%; mp 130.7-133.8 ºC. IR (KBr), (*v* max, cm^{-1}): 1597, 1562, 1469, 1426, 1398, 1363, 1286, 1235, 1204, 1163, 1074, 1063, 1011, 743. ^{1}H-NMR (400 MHz, DMSO-d_6): 9.18 (s, 1H, =CH), 8.18 (s, 1H, Ph-H), 8.10 (s, 1H, Thiazol-H), 8.04 (d, *J* = 8.0 Hz, 1H, Ph-H), 7.97 (d, *J* = 8.8 Hz, 2H, Ph-H), 7.71 (d, *J* = 8.8 Hz, 1H, Ph-H), 7.69 (d, *J* = 8.8 Hz, 2H, Ph-H), 7.63 (t, *J* = 8.0 Hz, 1H, Ph-H). ^{13}C-NMR (100 MHz, DMSO-d_6): 176.6 (Thiazol C=N), 168.4 (C=N), 156.6 (Thiazol), 142.0 (Ar-Cl), 139.1 (Ar), 138.4 (Ar), 137.8 (Ar), 137.0 (Ar), 136.3 (Ar), 134.2 (Ar), 133.5 (Ar), 133.2 (Ar), 126.7 (Ar-Br), 120.3 (Thiazol). MS (*m/z*, I%): 378 (M^+, 100%). Anal. Calcd for $C_{16}H_{10}BrClN_2S$ (377.69): C, 50.88%; H, 2.67%; N, 7.42%. Found: C, 50.92%; H, 2.67%; N, 7.45%.

4-Bromo-2-({[4-(4-hydroxyphenyl)thiazol-2-yl]imino}methyl)phenol (Z14)

Yellow solid; yield 58.4%; mp 224.3-227.1 ºC. IR (KBr), (*v* max, cm^{-1}): 3073, 1605, 1558, 1486, 1472, 1378, 1342, 1268, 1249, 1231, 1168, 1067, 742. ^{1}H-NMR (400 MHz, DMSO-d_6): 11.57 (s, 1H, -OH), 9.67 (s, 1H, -OH), 9.34 (s, 1H, =CH), 8.07 (s, 1H, Ph-H), 7.83 (s, 1H, Thiazol-H), 7.81 (d, *J* = 8.4 Hz, 1H, Ph-H), 7.63 (dd, *J* = 8.8 Hz, 2H, Ph-H), 7.71 (d, *J* = 8.8 Hz, 1H, Ph-H), 7.69 (d, *J* = 8.8 Hz, 2H, Ph-H), 7.63 (t, *J* = 8.8 Hz, 2.8 Hz, 1H, Ph-H), 7.01 (d, *J* = 8.8 Hz, 1H, Ph-H), 6.85 (d, *J* = 8.8 Hz, 2H, Ph-H). ^{13}C-NMR (100 MHz, DMSO-d_6): 170.9 (Thiazol C=N), 161.0 (C=N), 159.6 (Thiazol), 158.2 (Ar-Cl), 153.6 (Ar), 137.4 (Ar), 132.4 (Ar), 128.0 (Ar), 125.7 (Ar), 122.3 (Ar-Br), 119.7 (Ar), 118.0 (Ar), 111.8 (Ar), 111.3 (Thiazol). MS (*m/z*, I%): 374 (M^-, 100%). Anal. Calcd for $C_{16}H_{11}BrN_2O_2S$ (375.24): C, 51.21%; H, 2.95%; N, 7.47%. Found: C, 51.25%; H, 2.94%; N, 7.46%.

4-Chloro-2-({[4-(4-hydroxyphenyl)thiazol-2-yl]imino}methyl)phenol (Z15)

Yellow solid; yield 70.2%; mp 225.8-229.1 ºC. IR (KBr), (*v* max, cm^{-1}): 3075, 1608, 1560, 1488, 1378, 1345, 1269, 1249, 1233, 1168, 1067, 741. ^{1}H-NMR (400 MHz, DMSO-d_6): 11.56 (s, 1H, -OH), 9.69 (s, 1H, -OH), 9.34 (s, 1H, =CH), 7.92 (s, 1H, Thiazol-H), 7.81 (d, *J* = 6.8 Hz, 2H, Ph-H), 7.80 (s, 1H, Ph-H), 7.49 (dd, *J* = 7.2 Hz, 2.0 Hz, 1H, Ph-H), 7.05 (d, *J* = 7.2 Hz, 1H, Ph-H), 6.86 (d, *J* = 6.8 Hz, 2H, Ph-H). ^{13}C-NMR (100 MHz, DMSO-d_6): 170.5 (Thiazol C=N), 161.2 (C=N), 159.2 (Thiazol), 158.2 (Ar-OH),

153.5 (Ar-OH), 134.5 (Ar), 129.5 (Ar), 127.9 (Ar), 125.7 (Ar), 123.8 (Ar), 121.7 (Ar), 119.3 (Ar), 116.0 (Ar), 111.7 (Thiazol). MS (*m/z*, I%): 330 (M^-, 100%). Anal. Calcd for $C_{16}H_{11}ClN_2O_2S$ (330.79): C, 58.09%; H, 3.35%; N, 8.47%. Found: C, 58.11%; H, 3.38%; N, 8.45%.

4-{2-[(3,5-Dimethoxybenzylidene)amino]thiazol-4-yl}phenol (Z16)

Yellow solid; yield 32.2%; mp 194.2-196.4 °C. IR (KBr), (ν max, cm^{-1}): 3074, 1599, 1490, 1456, 1425, 1356, 1311, 1271, 1195, 1156, 1109, 840, 747. ^{1}H-NMR (400 MHz, DMSO-d_6): 9.68 (s, 1H, -OH), 9.08 (s, 1H, =CH), 7.82 (d, J = 6.8 Hz, 2H, Ph-H), 7.80 (s, 1H, Thiazol-H), 7.24 (s, 1H, Ph-H), 7.23 (s, 1H, Ph-H), 6.85 (d, J = 7.2 Hz, 1H, Ph-H), 6.74 (s, 1H, Ph-H), 3.83 (s, 6H, 2-OCH_3). ^{13}C-NMR (100 MHz, DMSO-d_6): 171.6 (Thiazol C=N), 164.2 (Ar-O-), 161.2 (C=N), 158.1 (Thiazol), 153.5 (Ar-OH), 137.2 (Ar), 127.9 (Ar), 125.8 (Ar), 116.0 (Ar), 111.4 (Thiazol), 107.6 (Ar), 105.8 (Ar), 56.0 (CH_3). MS (*m/z*, I%): 339 (M^-, 100%). Anal. Calcd for $C_{18}H_{16}N_2O_3S$ (340.40): C, 63.51%; H, 4.74%; N, 8.23%. Found: C, 63.55%; H, 4.76%; N, 8.22%.

Tyrosinase activity assay

Tyrosinase inhibition measurement was carried out according to our reported procedure.[24] Briefly, tyrosinase inhibitory activities of thiazol Schiff base derivatives were screened using *L*-DOPA as substrate. All the synthesized thiazol Schiff base derivatives and kojic acid were dissolved in DMSO. The DMSO stock solution of test compound was diluted with pH 6.8 phosphate buffer. Thirty units of mushroom tyrosinase (0.5 mg/mL) and the compounds, in 50 mM phosphate buffer (pH 6.8) were first pre-incubated for 10 min at 25 °C. 0.5 mM *L*-DOPA was added to the above mixture solution, and the enzyme reaction was continuously tracked by measuring change in absorbance at 475 nm of the Dopachrome formation with 1 min. The measurement was carried out in triplicate for each concentration, and the average value was used to further calculation. Kojic acid was used as a positive control compound, and the *o*-diphenolase inhibitory activities of the compounds were compared with kojic acid.

Inhibition mechanism of Z8 on the diphenolase activity of mushroom tyrosinase

The investigation of inhibitory type of selected compound **Z8** on mushroom tyrosinase was carried out according to reported protocol.[24] Compound **Z8** was used at the concentrations of 0 μM, 2 μM and 4 μM, respectively. Substrate *L*-DOPA concentration was between 500 μM and 1000 μM in the process of all kinetic study. Pre-incubation time and measurement time were the same as described in mushroom tyrosinase inhibition assay procedure. Lineweavere Burk plots of inverse of velocities (1/V) versus inverse of substrate concentration 1/[S] $\mu M^{-1}$was used to determine the type of enzyme inhibition.

In silico docking simulation of tyrosinase with compound Z8

To define the structure of the enzyme-inhibitor complex and to make sure accuracy, repeatability, and reliability of the docking results, AutoDock 4.2 program was used according to our reported process.[22] Among the many available molecular docking tools, AutoDock 4.2 is the most commonly used because

of its automatic docking function. Crystal structure of tyrosinase (PDB code: 2Y9X) was got from the Protein DataBank (http://www.rcsb.org, Rutgers and UCSD/SDSC). We performed simulations of the docking tyrosinase with compound **Z8**. To prepare the docking simulation of compound **Z8**, the following three steps were carried out: (1) 2D structure was converted to 3D structure, (2) charges were counted, and (3) hydrogen atoms were added with the ChemBioOffice program (http://www.cambridgeoft.com).

Fluorescence measurements

To investigate fluorescence quenching role of inhibitor to the tyrosinase, fluorescence experiments were carried according to the reported method.[23] To determine the linear concentration range of the fluorescence, compound **Z8** was first dissolved in DMSO. The concentration of the solution was 1.0 mM, and then was diluted with sodium phosphate buffer. The ultimate concentration was changed from 0 to 100 μM. A series of 2.5 mL solutions containing 0.2 mL of tyrosinase solution were added to a centrifuge tube and then accurately mixed with different concentrations of **Z8** solution range from 0 to 100 μM. Cary Eclipse G9800A fluorescence spectrophotometer (Agilent Technologies Co) was employed to detect the fluorescence intensity. The excitation wavelength was set to 280 nm, the bath was set as two temperatures (288 and 303 K) with a scanning wavelength change from 295 to 525 nm. The excitation and emission bandwidths were 5 nm. The final tyrosinase concentration was 0.1 mg/mL.

Effects on the browning process of fresh-cut apples and potato assay

Fuji apples were planted in Yantai of Shandong province, China, and were bought from Walmart supermarket in Shaoyang, Hunan Province, China. The apples were come from the same batch having similar shapes, maturity, and without injuries, rot, diseases or pests. Potato was also bought from Walmart supermarket in Shaoyang, Hunan Province, China. Apples and potato were cut into thin pieces with same size by using a sharp knife. Then, the fresh-cut slices were divided randomly into different groups: blank control group was immersed in ethanol for 10 min at room temperature, treatment groups were dipped in the solution of compound **Z8** under the same conditions, positive groups were dipped in 40 μM kojic acid and 20 μM Vc under the same conditions. The test samples were air-dried naturally and immediately were separately packaged with polyethylene clam-packs, and stored at 5 °C, and used for the following experimental measurements.

According to the reported protocol,[25] the color of apple and potato samples were tested by a CR-400 Minolta chronometer instrument (Konica Minolta, Osaka, Japan). Three data of L^*, a^*, and b^* were recorded for each sample. The L^* values indicate lightness, the a^* values show reddish-greenish, the b^* values represent yellowish-bluish. The color measurement was carried out in triplicate by random sampling.

ACKNOWLEDGMENT

This work was supported by the Science Foundation of Education Department of Hunan Province, China (19C1632).

SUPPORTING INFORMATION

Supplementary (^{1}H- and ^{13}C-NMR spectra) data associated with this article can be found, in the online version, at URL: https://www.heterocycles.jp/newlibrary/downloads/PDFsi/27251/102/7.

REFERENCES

1. Z. Dehghani, M. Khoshneviszadeh, and S. Ranjbar, *Bioorg. Med. Chem.*, 2019, **27**, 2644.
2. Á. Sánchez-Ferrer, J. N. Rodríguez-López, F. García-Cánovas, and F. García-Carmòna, *Biochim. Biophys. Acta*, 1995, **1247**, 1.
3. L. Ielo, B. Deri, M. P. Germanò, S. Vittorio, S. Mirabile, R. Gitto, A. Rapisarda, S. Ronsisvalle, S. Floris, Y. Pazy, A. Fais, A. Fishman, and L. D. Luca, *Eur. J. Med. Chem.*, 2019, **178**, 380.
4. Y. Nazir, A. Saeed, M. Rafiq, S. Afzal, A. Ali, M. Latif, J. Zuegg, W. M. Hussein, C. Fercher, R. T. Barnard, M. A. Cooper, M. A. T. Blaskovich, Z. Ashraf, and Z. M. Ziora, *Bioorg. Med. Chem. Lett.*, 2020, **30**, 126722.
5. M. Brenner and V. J. Hearing, *Photochem. Photobiol.*, 2008, **84**, 539.
6. S. Chortani, V. D. Nimbarte, M. Horchani, H. B. Jannet, and A. Romdhane, *Bioorg. Chem.*, 2019, **92**, 103270.
7. T. Oyama, S. Takahashi, A. Yoshimori, T. Yamamoto, A. Sato, T. Kamiya, H. Abe, T. Abe, and S. Tanuma, *Bioorg. Med. Chem.*, 2016, **24**, 4509.
8. T. Pillaiyar, M. Manickam, and V. Namasivayam, *J. Enzym. Inhib. Med. Chem.*, 2017, **32**, 403.
9. P. G. Mahajan, N. C. Dige, B. D. Vanjare, H. Raza, M. Hassan, S. Y. Seo, C. H. Kim, and K. H. Lee, *J. Mol. Struct.*, 2019, **1198**, 126915.
10. Q. Yu, L. Fan, and Z. Duan, *Food Chem.*, 2019, **297**, 124910.
11. S. Ghafary, S. Ranjbar, B. Larijani, M. Amini, M. Biglar, M. Mahdavi, M. Bakhshaei, M. Khoshneviszadeh, A. Sakhteman, and M. Khoshneviszadeh, *Int. J. Biol. Macromol.*, 2019, **135**, 978.
12. M. D. Santi, M. A. Peralta, M. Puiatti, J. L. Cabrera, and M. G. Ortega, *Bioorg. Med. Chem.*, 2019, **27**, 3722.
13. S. Radhakrishnan, R. Shimmon, C. Conn, and A. Baker, *Bioorg. Chem.*, 2015, **62**, 117.
14. S. Lee, S. Ullah, C. Park, H. W. Lee, D. Kang, J. Yang, J. Akter, Y. Park, P. Chun, and H. R. Moon, *Bioorg. Med. Chem.*, 2019, **27**, 3929.
15. S. Garg and N. Raghav, *Asian J. Pharm. Clin. Res.*, 2013, **6**, 181.

16. M. S. Salem, R. A. Hussein, and W. M. El-Sayed, *Anti-Cancer Agents Med. Chem.*, 2019, **19**, 620.
17. C. P. V. Mary, R. Shankar, and S. Vijayakumar, *Mol. Simulat.*, 2019, **45**, 636.
18. F. Ali, K. M. Khan, U. Salar, M. Taha, N. H. Ismail, A. Wadood, M. Riaz, and S. Perveen, *Eur. J. Med. Chem.*, 2017, **138**, 255.
19. S. Carradori, D. Rotili, C. D. Monte, A. Lenoci, M. D'Ascenzio, V. Rodriguez, P. Filetici, M. Miceli, A. Nebbioso, L. Altucci, D. Seccia, and A. Mai, *Eur. J. Med. Chem.*, 2014, **80**, 569.
20. W. Xie, Y. Wu, J. Zhang, Q. Mei, Y. Zhang, N. Zhu, R. Liu, and H. Zhang, *Eur. J. Med. Chem.*, 2018, **145**, 35.
21. N. R. Filipović, H. Elshaflu, S. Grubišić, L. S. Jovanović, M. Rodić, I. Novaković, A. Malešević, I. S. Djordjević, H. Li, N. Šojić, A. Marinković, and T. R. Todorović, *Dalton Trans.*, 2017, **46**, 2910.
22. J. Tang, J. Liu, and F. Wu, *Bioorg. Chem.*, 2016, **69**, 29.
23. H. Hridya, A. Amrita, S. Mohan, M. Gopalakrishnan, T. K. Dakshinamurthy, G. P. Doss, and R. Siva, *Int. J. Biol. Macromol.*, 2016, **86**, 383.
24. J. Liu, W. Yi, Y. Wan, L. Ma, and H. Song, *Bioorg. Med. Chem.*, 2008, **16**, 1096.
25. J. Wu, K. Cheng, E. T. S. Li, M. Wang, and W. Ye, *Food Chem.*, 2008, **109**, 379.